

Neural Observer Based Hybrid Intelligent Scheme for Activated Sludge Wastewater Treatment

E. A. Hernandez-Vargas,^{a,*} E. N. Sanchez,^a J. F. Beteau,^b and C. Cadet^b

^aCINVESTAV, Unidad Guadalajara, Departamento de Control Automatico, Apartado Postal 31-438, Plaza la Luna, Guadalajara, Jal. Mexico, 45090

^bInstitute National Polytechnique de Grenoble, GIPSA-lab Department of control systems BP 46-38402 St-Martin d'Hères Cedex, France

Original scientific paper

Received: June 2, 2008

Accepted: February 17, 2009

Activated sludge wastewater treatment plants have received considerable attention due to their efficiency to eliminate biodegradable pollution and their robustness to reject disturbances. Different control strategies have been proposed, but most of these techniques need sensors to measure process main variables. This paper presents a discrete-time recurrent high order neural observer (RHONO) to estimate substrate and biomass concentrations in an activated sludge wastewater treatment plant. The RHONO is trained on-line with an extended Kalman filter (EKF)-based algorithm. Then this observer is associated with a hybrid intelligent system based on fuzzy logic to control the substrate/biomass concentration ratio using the external recycle flow rate and the injected oxygen as control actions. The intelligent system and neural observer performance is illustrated via simulations.

Key words:

Wastewater treatment, neural observer, process control, hybrid intelligent control

Introduction

The use of wastewater treatment plants (WWTPs) has increased due to environmental issues. Regarding this fact, wastewater treatment plants based on activated sludge technology are suitable for urban wastewater. In addition, these plants are used due to their efficiency to treat water and their capacity to work under disturbances.

Controlling a WWTP is a difficult task, and different strategies should be implemented in order to maintain good operations conditions in presence of external disturbances. Some authors have proposed different control schemes (Olsson *et al.*,¹ Brdys *et al.*² and Vera *et al.*³). These approaches make an effort to keep the quality of the effluent, while others try to minimize energy (Tong *et al.*⁴).

However, the application of these strategies requires sensors allowing the measurements of the process main variables; these sensors could be very expensive and require elaborated maintenance procedure. Due to these facts, state estimation applied to WWTP has received special attention by many authors, who have obtained interesting results in different directions and for different purposes. Most of the existing results need the use of a special non-linear transformation (Lopez *et al.*⁵). Other kinds of

observers are those called robust, which have good performance under uncertainties although their design is too complex and has very restrictive conditions (Alcaraz *et al.*⁶). The main problem of all the approaches mentioned above is the requirement to know at least partially the plant dynamic model. However, other kinds of observers have been recently proposed: neural observers (Poznyak *et al.*,⁷ Sanchez *et al.*⁸ and Rovithakis⁹) which do not need this requirement.

This paper is related to two main aspects: 1) the development of the recurrent high order neural observer (RHONO), based on a RHONN (Rovithakis⁹) which is applied to a WWTP in order to estimate the substrate and biomass concentration using dissolved oxygen as the measured variable. The neural observer learning uses an extended Kalman filter algorithm (Sanchez *et al.*¹⁰). 2) Furthermore, we associate this neural observer to an intelligent control, which uses fuzzy logic to regulate the substrate/biomass concentration ratio, in order to ensure effluent quality even in the presence of external disturbances.

Process description

The process of a typical aerobic treatment plant corresponds to the benchmark of the European group COST 624 (Beteau *et al.*¹¹); the diagram of the

* Author to whom all correspondence should be addressed, e-mail: abelardo_81@hotmail.com, Tel: (52) 33 3777 3600 ext. 1009.

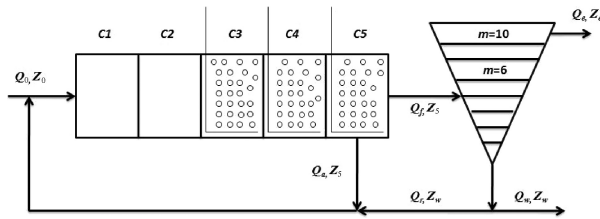


Fig. 1 – Activated sludge wastewater process scheme

aerobic treatment plant is presented in Fig. 1. The two main parts are: the bioreactor which usually can be modeled by five perfectly mixed tanks, and the settler modeled with 10 layers (Takacs *et al.*¹²).

The first two compartments of the bioreactor are non-aerated and there denitrification takes place; the next three compartments (nitrification process) are aerated. Q_0 and Z_0 are respectively the flow rate and the concentrations of the plant influent (disturbances); Q_f and Z_5 are the flow rate and concentration at the bioreactor output; Q_e and Z_e are the flow rate and concentration of the plant effluent; Q_w and Z_w are the flow rate and concentration of the sludge wastage; Q_r is the external recycle flow rate and Q_a is the internal recycle flow rate. The global mathematical model for this process requires 145 nonlinear differential equations, obtained by calculating mass balances for the 5 sections of the bioreactor and the 10 layers of the settler. Benchmark simulations are implemented with the simulator provided in (Betau *et al.*¹¹). All flow rates used in the model are in $\text{m}^3 \text{d}^{-1}$. Kinetic parameters, constants and control scenarios, were taken from (Betau *et al.*¹¹). The process model uses 13 state variables in accordance with ASM1. The main variables are:

- γ_s – fast biodegradable substrate
- γ_{BH} – active heterotrophic biomass
- γ_{BA} – active autotrophic biomass
- γ_{O_2} – dissolved oxygen
- γ_{NO} – nitrate and nitrite nitrogen
- γ_{NH} – ammoniacal nitrogen

Discrete-time recurrent high order neural network

Let us consider a MIMO nonlinear system

$$x_i(k+1) = F(x(k), u(k)) \quad (1)$$

where $x \in R^n$, $u \in R^m$ and $F \in R^n \times R^m \rightarrow R^n$ is a nonlinear function. Now a discrete-time recurrent high order neural network (RHONN) may be described as:

$$x_i(k+1) = w_i^T z_i(x(k), u(k)), \quad i = 1, \dots, n \quad (2)$$

where x_i ($i = 1, 2, \dots, n$) is the state of the i -th neuron, L_i is the respective number of higher-order connections, n is the state dimension, $\{I_1, I_2, \dots, I_{L_i}\}$ is a collection of non-ordered subsets of $\{1, 2, \dots, n\}$, w_i ($i = 1, 2, \dots, n$) is the respective on-line adapted weight vector, and $z_i(x(k), u(k))$ is given by

$$z_i(x(k), u(k)) = \begin{bmatrix} z_{i_1} \\ z_{i_2} \\ \vdots \\ z_{i_{L_i}} \end{bmatrix} = \begin{bmatrix} \pi_{j \in I_1} y_i^{d_{j(1)}} \\ \pi_{j \in I_2} y_i^{d_{j(2)}} \\ \vdots \\ \pi_{j \in I_{L_i}} y_i^{d_{j(L_i)}} \end{bmatrix} \quad (3)$$

with $d_{j_i}(k)$ non-negative integers and y_i defined as follows:

$$y_i = \begin{bmatrix} y_{i_1} \\ \vdots \\ y_{i_i} \\ y_{i_n} \\ \vdots \\ y_{i_{n+m}} \end{bmatrix} = \begin{bmatrix} S(x_1) \\ \vdots \\ S(x_n) \\ u_1 \\ \vdots \\ u_m \end{bmatrix} \quad (4)$$

In (4), $u = [u_1, u_2, \dots, u_m]^T$ is the input vector to the neural network (NN), and $S(\bullet)$ is defined as

$$S(x) = \frac{1}{1 + \exp(-\beta x)} + \varepsilon \quad (5)$$

We consider now the problem to approximate the general-time nonlinear system (1), by the following discrete-time RHONN:

$$x_i(k+1) = w_i^{*T} z_i(x(k), u(k)) + \varepsilon_{z_i}, \quad i = 1, \dots, n \quad (6)$$

where x_i is the i -th plant state, ε_{z_i} is the bounded approximation error, which may be reduced by increasing the number of adjustable weights (Rovithakis⁹). Assume that there exists ideal weight vector w_i^* such that $\|\varepsilon_{z_i}\|$ can be minimized on a compact set $\Omega_{z_i} \subset R^{L_i}$. In general, it is assumed that this vector exists and is constant but unknown. Let us define its estimate as w_i and the estimation error as

$$\hat{w}_i(k) = w_i^* - w_i(k) \quad (7)$$

EKF training algorithm

For EKF-based neural network training, the network weights become the states to be estimated. In this case, the error between the neural network output and the measured plant output can be considered as additive white noise. Because neural network mapping is nonlinear, an EKF is required. The

training goal is to find the optimal weight values to minimize the prediction error (Song *et al.*¹³). In this work, we used an EKF-based training algorithm described by

$$\begin{aligned} w_i(k+1) &= w_i(k) + \eta_i K_i(k) e_i(k) \\ K_i(k) &= P_i(k) H_i(k) M_i(k) \quad i = 1, \dots, n \quad (8) \\ P_i(k+1) &= P_i(k) - K_i(k) H_i^T(k) P_i(k) + Q_i(k) \end{aligned}$$

with

$$\begin{aligned} M_i(k) &= [R_i(k) + H_i^T(k) P_i(k) H_i(k)]^{-1} \\ e_i(k) &= y(k) - \hat{y}(k) \end{aligned} \quad (9)$$

where $e(k) \in R^p$ is the observation error and $P_i(k) \in R^{L_i \times L_i}$ is the weight estimation error covariance matrix at step k , $w_i \in R^{L_i}$ is the weight (state) vector, L_i is the respective number neural network weights, $y \in R^p$ is the plant output, $\hat{y} \in R^p$ is the NN output, n is the number of states, $K_i \in R^{L_i \times p}$ is the Kalman gain matrix, $Q_i \in R^{L_i \times L_i}$ is the NN weight estimation noise covariance matrix, $R_i \in R^{p \times p}$ is the error noise covariance, and $H_i \in R^{L_i \times p}$ is a matrix, in which each entry (H_{ij}) is the derivative of the i -th neural output with respect to ij -th NN weight, (w_{ij}), given as follows:

$$H_{ij}(k) = \left[\frac{\partial \hat{y}(k)}{\partial w_{ij}(k)} \right]^T \quad (10)$$

where $i = 1, \dots, n$ and $j = 1, \dots, L_i$. Usually P_i and Q_i are initialized as diagonal matrices, with entries $P_i(0)$ and $Q_i(0)$, respectively. It is important to note that $H_i(k)$, $K_i(k)$ and $P_i(k)$ for the EKF are bounded; for a detailed explanation of this fact see (Song *et al.*¹³). To obtain H in (10) is not an easy task. In this case $\hat{y}(k) = x_i(k)$, so by the chain rule, we have

$$\frac{\partial \hat{y}(k)}{\partial w_{ij}(k)} = \frac{\partial \hat{y}(k)}{\partial x_i(k)} \frac{\partial x_i(k)}{\partial w_{ij}(k)} \quad (11)$$

Discrete-time neural observer

In this section, we briefly present the neural observer, proposed in (Sanchez *et al.*⁸). We consider the state of a discrete-time nonlinear system, which is assumed observable, given by

$$\begin{aligned} x(k+1) &= F(x(k), u(k)) + d(k) \\ y(k) &= Cx(k) \end{aligned} \quad (12)$$

where $x \in R^n$ is the state vector of the system, $u \in R^m$ is the input vector, $y(k) \in R^p$ is the output vector, $C \in R^{p \times n}$ is a known output matrix, $d(k) \in R^n$ is a

disturbance vector and $F(\bullet)$ is a smooth vector field and $F_i(\bullet)$ its entries; hence (12) can be rewritten as:

$$\begin{aligned} x(k+1) &= [x_1(k) \dots x_i(k) \dots x_n(k)]^T \\ d(k) &= [d_1(k) \dots d_i(k) \dots d_n(k)]^T \\ x_i(k+1) &= F_i(x(k), u(k)) + d_i(k), \quad i = 1, \dots, n \\ y(k) &= Cx(k) \end{aligned} \quad (13)$$

For system (13), a Luenberger neural observer (RHONO) is proposed with the following structure:

$$\begin{aligned} \hat{x}(k) &= [\hat{x}_1(k) \dots \hat{x}_i(k) \dots \hat{x}_n(k)]^T \\ \hat{x}_i(k+1) &= w_i^T z_i(\hat{x}(k), u(k)) + L_i e(k) \\ \hat{y}(k) &= C\hat{x}(k), \quad i = 1, \dots, n \end{aligned} \quad (14)$$

with $\hat{x} \in \mathfrak{R}^n$, $\hat{y} \in \mathfrak{R}^p$ the state and output estimates respectively, $L_i \in R^p$, w_i and z_i as in (2); the weight vectors are updated on-line with a decoupled EKF (8)–(11). The output error is defined by

$$e(k) = y(k) - \hat{y}(k) \quad (15)$$

and the state estimation error as

$$\tilde{x}(k) = x(k) - \hat{x}(k) \quad (16)$$

Hence, the dynamics of (16) can be expressed as

$$\begin{aligned} \tilde{x}(k+1) &= x_i(k+1) - \hat{x}_i(k+1) = \\ &= w_i^{*T} z_i(x(k), u(k)) + \varepsilon_{z_i} + d_i(k) - \\ &\quad - w_i^T z_i(\hat{x}(k), u(k)) - L_i e(k) = \\ &= \hat{w}_i z_i(\hat{x}(k), u(k)) + \varepsilon_{z_i} + d_i(k) - L_i e(k) \end{aligned} \quad (17)$$

The stability properties at such observer are stated in the following theorem:

Theorem 1: For the system (13) the RHONO (14), trained with the EKF-based algorithm, ensures that the estimation error (16) and the output error (15) are semiglobally uniformly ultimately bound; moreover, the RHONO weights remain bounded. For proof, see (Sanchez *et al.*⁸).

Considering (14) and (15)

$$e(k) = C\tilde{x}(k) \quad (18)$$

Then the error of (9) can be rewritten as

$$\tilde{x}(k+1) = \hat{w}_i z_i(\hat{x}(k), u(k)) + \varepsilon'_{z_i} - L_i C\tilde{x}(k) \quad (19)$$

where $\varepsilon'_{z_i} = \varepsilon_{z_i} + d_i(k)$. On the other hand the dynamics of (9) is

$$\hat{w}_i(k+1) = w_i^* - w_i(k+1) = \hat{w}_i(k) - \eta_i K_i(k) e(k) \quad (20)$$

Observer application to WWTP

To this end, the neural observer is applied to a WWTP, whose nonlinear dynamics is considered unknown. To estimate substrate and biomass concentrations with oxygen concentration measurement in the fifth compartment of the bioreactor, we use the RHONO (13) with $n = 3$. The used neural observer has the following structure:

$$\hat{x}_1(k+1) = w_{11}S(\hat{x}_1) + w_{12}S(\hat{x}_1)^2 S(\hat{x}_2)S(\hat{x}_3) + w_{13}S(\hat{x}_3) + w_{14}S(u_1)$$

$$\hat{x}_2(k+1) = w_{21}S(\hat{x}_2) + w_{22}S(\hat{x}_1)^2 S(\hat{x}_2)S(\hat{x}_3)^3 + w_{23}S(\hat{x}_2) + w_{24}u_2$$

$$\hat{x}_3(k+1) = w_{31}S^2(\hat{x}_3) + w_{32}S(\hat{x}_1)^2 S^2(\hat{x}_2)S(\hat{x}_3)^3 + w_{33}S(\hat{x}_3) + w_{34}S(u_3)$$

$$\hat{y} = \hat{x}_3$$

where \hat{x}_1 , \hat{x}_2 and \hat{x}_3 are the estimates of the fast biodegradable substrate (γ_S), active heterotrophic biomass (γ_{BH}) and oxygen (γ_{O_2}), respectively. The input u_1 is the flow rate of the plant influent Q_0 , u_2 is the external recycle flow rate Q_r , and u_3 is the control action for oxygen in the fifth compartment bioreactor. The observer scheme is presented in Fig. 2.

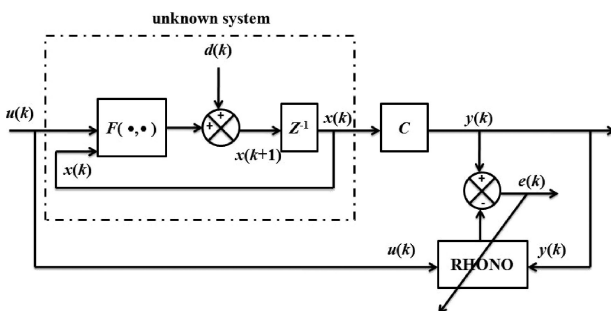


Fig. 2 – Observation scheme

The training was performed on-line, using a parallel configuration. All the NN states were initialized randomly. The sampling period was based on dissolved oxygen measurements, acquired every seven minutes. The covariance matrices were initialized as diagonal, with nonzero elements as: $P_i(0) = 800000$, $Q_i(0) = 200$ and $R_i(0) = 4000$, ($i = 1,2,3$), respectively.

Simulation results

For simulation, the scenario considered was: for first four days a constant disturbance was included; finally for the next days a time variable disturbance was inserted, as displayed in Fig. 3.

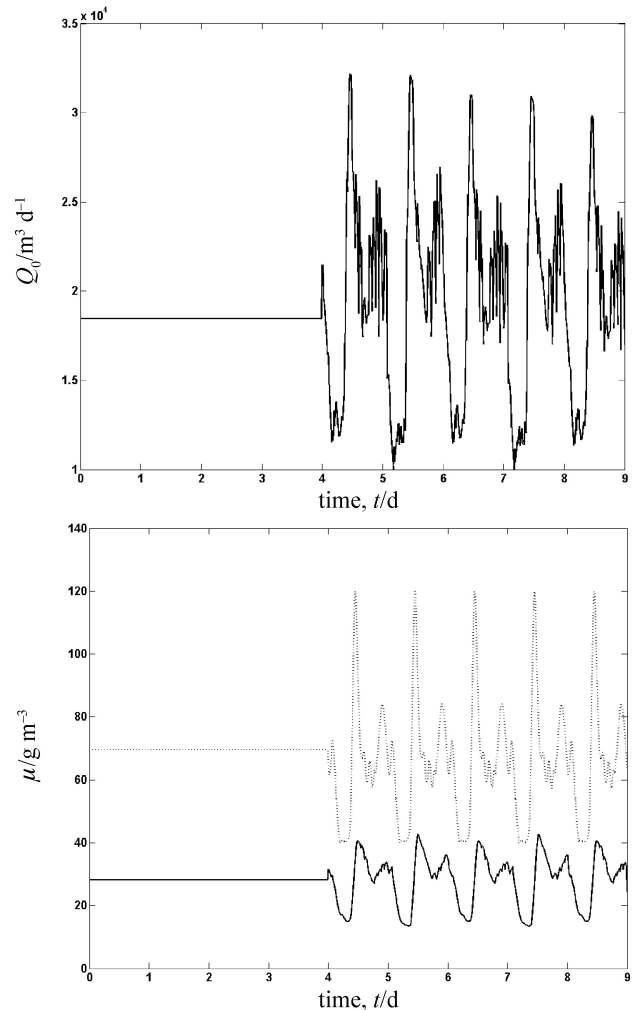


Fig. 3 – External disturbance: (a) Volumetric flux influent; (b) Fast biodegradable substrate (solid line) and heterotrophic biomass concentrations influent (dashed line)

As may be seen in Fig. 4, exact convergence is obtained for the state variable (γ_{O_2}) as expected, whereas for the other state variables good estimations are achieved.

Control strategy

L/A structure

This structure is discussed in (Vera *et al.*³) and portrayed in Fig. 5, which is called *L/A* because two transformations are used; the first one is based on the logarithmic (*L*) function and the second one on the antilogarithmic (*A*) function, as follows:

Logarithm

$$Y(t) = \ln y(t)$$

$$Y^*(t) = \ln y^*(t) \quad (21)$$

$$U(t) = \ln u(t)$$

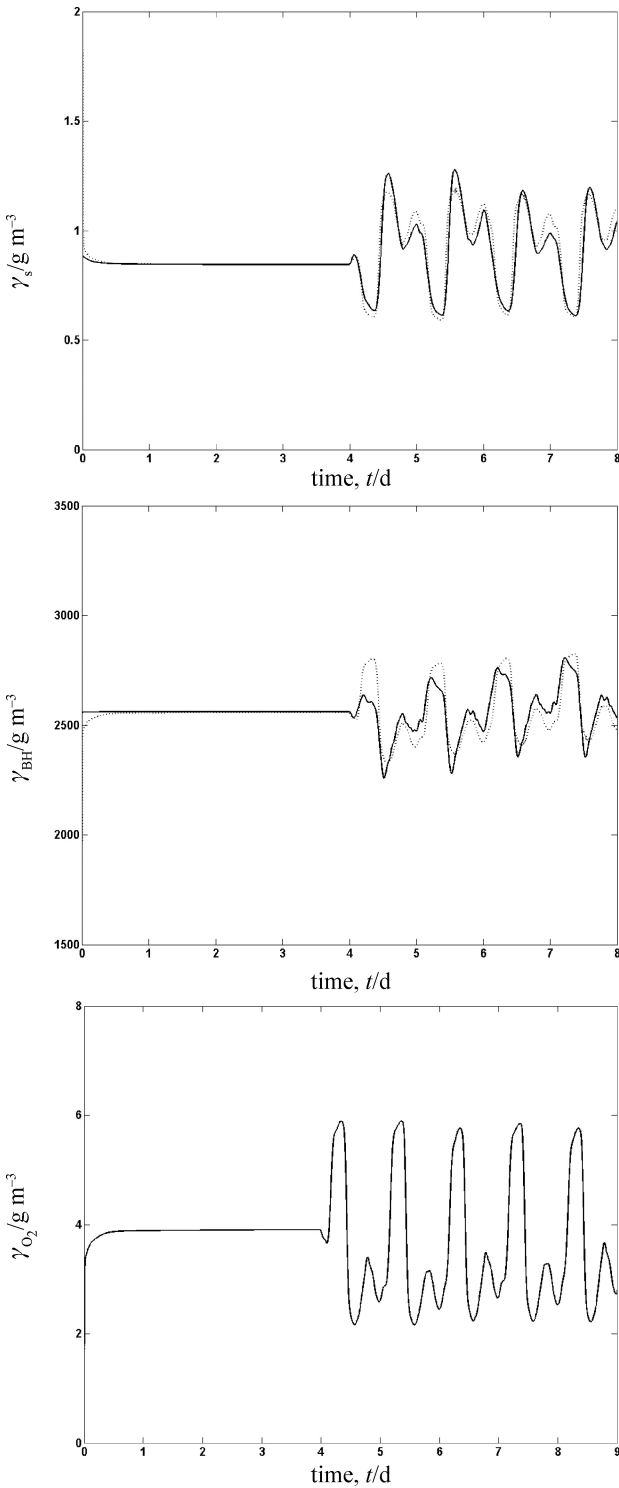


Fig. 4 – Fast biodegradable substrate, heterotrophic biomass and oxygen concentrations (solid line) and their respective estimates (dashed line)

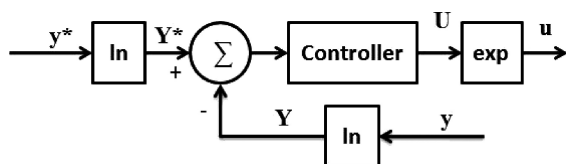


Fig. 5 – L/A controller

Antilogarithm

$$y(t) = \exp Y(t)$$

$$y^*(t) = \exp Y^*(t) \tag{22}$$

$$u(t) = \exp U(t)$$

where $y(t)$ is the output, $y^*(t)$ is the set point, and $u(t)$ is the control action. These transformations allow to select any conventional control law and to obtain an L/A equivalent.

Fuzzy supervisory control

The Takagi – Sugeno system is a special case of “functional fuzzy systems”:

$$\begin{aligned} \text{If } u_1 \text{ is } A_1^j \text{ and } u_2 \text{ is } A_2^j \text{ and, } \dots, \\ \text{and } u_n \text{ is } A_n^j \text{ then } b_i = g_i(\cdot) \end{aligned} \tag{23}$$

where (\cdot) represents the arguments of the function g_i . The premise of this rule is defined with linguistic terms like for the standard fuzzy system. The consequent is different; instead of linguistic terms with an associated membership function, we use a function $b_i = g(\cdot)$, which does not have an associated membership function. The choice of this function depends on the application being considered. Virtually any function can be used (e.g. a linear equation, neural network mapping or another fuzzy system), which makes the functional fuzzy system very general. The functional fuzzy system can use an appropriate logical operation for representing the premise (e.g., minimum or product) and defuzzification may be obtained using

$$y = \frac{\sum_{i=1}^R b_i \mu_i}{\sum_{i=1}^R \mu_i} \tag{24}$$

where μ_i is the membership value defined as

$$\mu_1(u_1, u_2, \dots, u_n) = \mu_{A_1^j}(u_1) * \mu_{A_2^k}(u_2) * \dots * \mu_{A_n^l}(u_n)$$

One way to view the functional fuzzy system is as a nonlinear interpolation between the mappings that are defined by consequents of the rules. When the consequent function is a linear one, the functional fuzzy system is named as a Takagi-Sugeno one (Passino¹⁴), such as

$$b_i = g_i(\cdot) = a_{i,0} + a_{i,1}\mu_1 + \dots + a_{i,n}u_n$$

where $a_{i,j}$ are real numbers.

Hybrid intelligent scheme

For this strategy, we use fast biodegradable substrate and heterotrophic biomass concentrations, estimated by the proposed neural observer scheme. This strategy is based on the following reasoning: if there is an excessive amount of biomass concentration, then the suspended solids increase. If the biomass concentration is low and substrate concentration is high, influent pollution cannot be treated. Both cases degrade treated water quality. For these reasons, we propose a relation RT , which has to be kept constant;

$$RT = \frac{\gamma_{BH}}{\gamma_s} \tag{25}$$

The hybrid intelligent control is based on RT regulation, using the scheme shown in Fig. 6; in this scheme, a PI L/A controller is considered to control γ_{O_2} using as manipulated variable $k_L a$ (aeration constant); for a detailed explanation see (Vera et al.⁷).

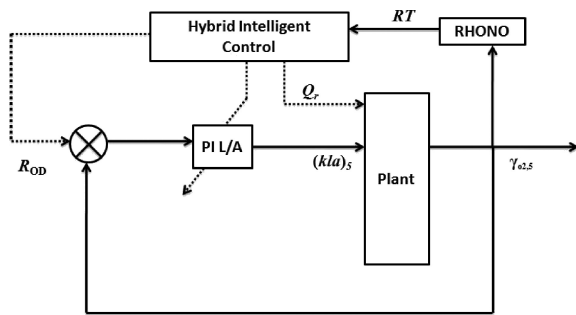


Fig. 6 - Hybrid intelligent control scheme

The structure of the hybrid intelligent scheme uses a fuzzy supervisor to modify the oxygen set point (R_{OD}) and the external recycle flow rate Q_r . The respective fuzzy sets are defined as in Fig. 7.

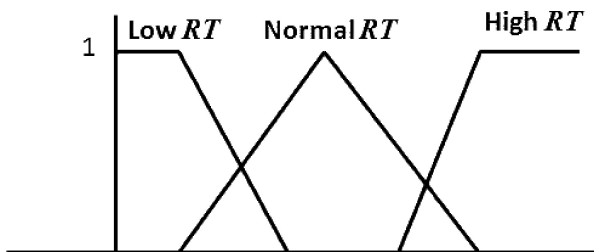


Fig. 7 - Input membership functions

The respective rules are:

- If RT is low then $Q_r = Q_{rl}$ and $R_{OD} = R_l$
- If RT is normal then $Q_r = Q_{rn}$ and $R_{OD} = R_n$
- If RT is high then $Q_r = Q_{rh}$ and $R_{OD} = R_h$

Fig. 8 and Fig. 9 display how the proposed hybrid intelligent control keeps both outputs: the oxygen (γ_{O_2}) and the ratio RT at the designed values when there is a constant external disturbance. When this disturbance is time varying, the control is still able to keep these outputs around the desired values. Fig. 10 presents the time-evolution for the estimation of fast biodegradable and heterotrophic biomass concentration. This estimation performs adequately.

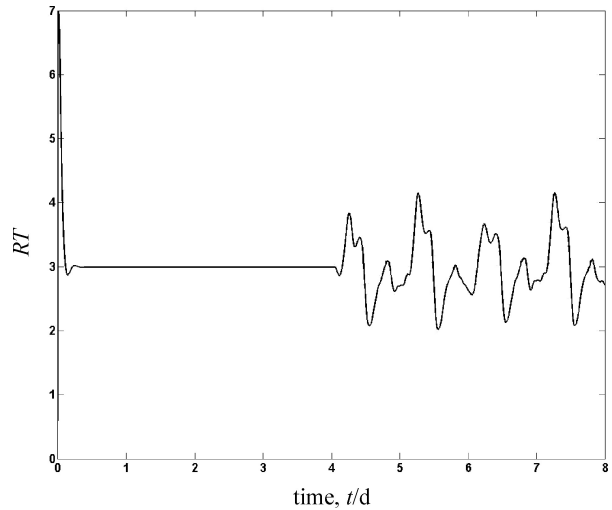


Fig. 8 - RT Tracking using intelligent control

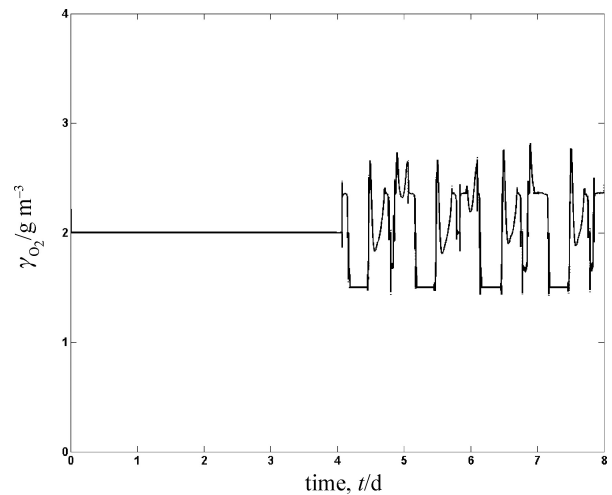


Fig. 9 - Oxygen dissolved concentration (solid line) and their respective estimates (dashed line)

Quality improvements and cost reduction

This control strategy, in addition to ensure good operational conditions, improves the effluent quality in three aspects: total suspended solids, chemical oxygen demand and biological oxygen demand. The reduction of the total suspended solids may be seen in Fig. 11.

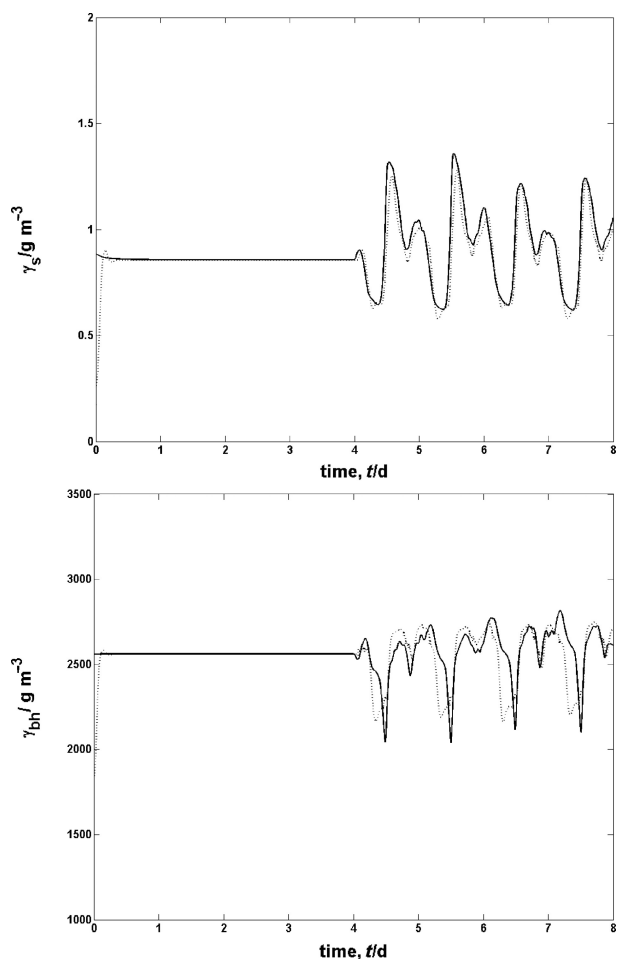


Fig. 10 – Fast biodegradable substrate and heterotrophic biomass concentrations (solid line) and their respective estimates (dashed line)

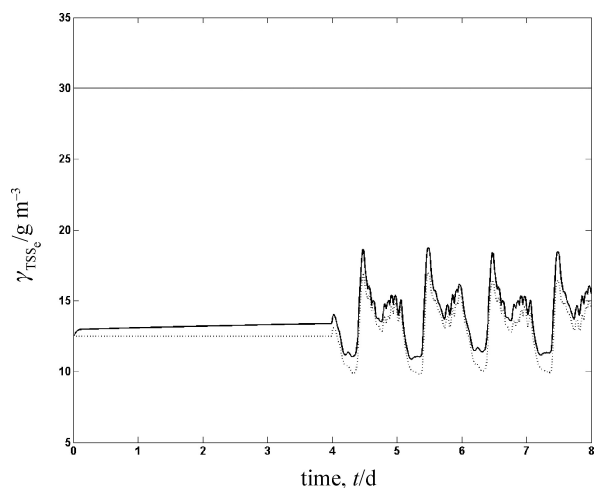


Fig. 11 – Total suspended solids concentration under control actions (solid line) and in open loop (dashed line); the horizontal line is the highest value admitted by the quality norm

Additionally the total suspended solids reduction, there is also a reduction for the chemical oxygen demand, see Fig. 12 and for the biological oxygen demand, as is shown in Fig. 13. The plant in

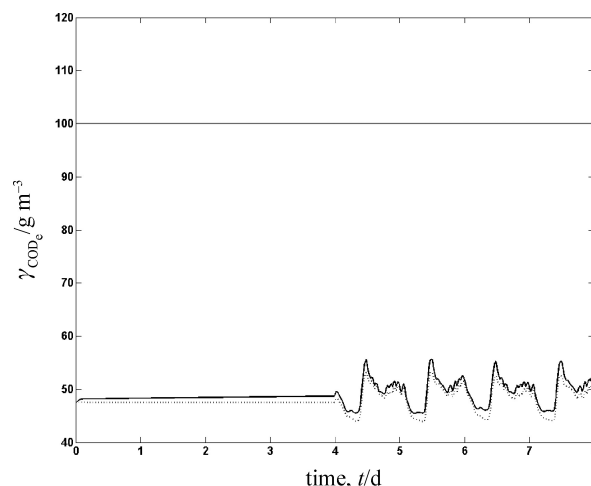


Fig. 12 – Chemical oxygen demand concentration under control actions (solid line) and in open loop (dashed line); the horizontal line is the highest value admitted by the quality norm

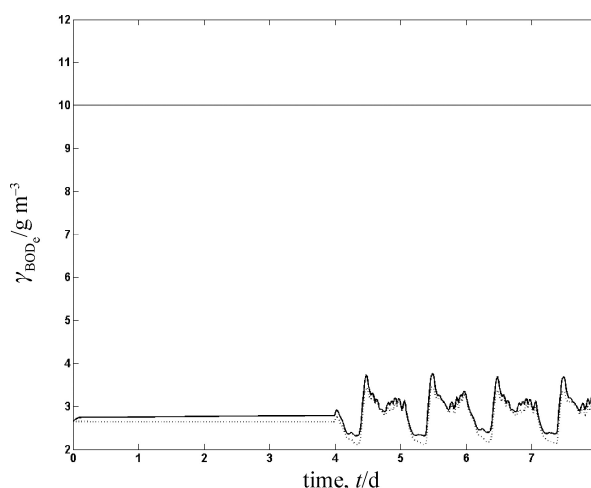


Fig. 13 – Biological oxygen demand concentration under control actions (solid line) and in open loop (dashed line); the horizontal line is the highest value admitted by the quality norm

open loop also ensures good quality; this is due to the plant is operated at the maximum oxygenation and recirculation flows. For this reason, plant costs are high. It is possible to verify that the proposed control strategy reduces the plant energy consumption, as displayed in Table 1.

Table 1 – Energy consumption

	Open loop	Control strategy	Energy savings
	$P/\text{kW d}^{-1}$	$P/\text{kW d}^{-1}$	%
aeration energy	7533	6248	17
pumping energy	3629	3025	20

Conclusions

In this paper, the estimation of fast biodegradable substrate and heterotrophic biomass concentration, in a WWTP has been implemented, using a RHONO and considering only on-line measurements of the dissolved oxygen. Simulation results illustrate the effectiveness of the observer even in presence of input disturbances. Additionally, the proposed fuzzy supervisor allows regulating the substrate/biomass ratio. The whole hybrid intelligent scheme provides a reduction on energy costs and promising guidelines to tackle the problem of WWTP control.

ACKNOWLEDGMENT

The authors thank the support of CONACYT Mexico Project 57801Y.

List of symbols

a	– real numbers
Q_0	– flow rate of the plant influent, $\text{m}^3 \text{d}^{-1}$
Q_f	– flow rate at the bioreactor output, $\text{m}^3 \text{d}^{-1}$
Q_e	– flow rate of the plant effluent, $\text{m}^3 \text{d}^{-1}$
Q_w	– flow rate of the sludge wastage, $\text{m}^3 \text{d}^{-1}$
Q_r	– external recycle flow rate, $\text{m}^3 \text{d}^{-1}$
Q_a	– internal recycle flow rate, $\text{m}^3 \text{d}^{-1}$
Z_0	– concentration of the plant influent
Z_5	– concentration at the bioreactor output
Z_e	– concentration of the plant effluent
Z_w	– concentration of the sludge wastage
γ_S	– fast biodegradable substrate, g m^{-3}
γ_{BH}	– active heterotrophic biomass, g m^{-3}
γ_{BA}	– active autotrophic biomass, g m^{-3}
γ_{O_2}	– dissolved oxygen, g m^{-3}
F	– nonlinear function
x	– plant state vector
\hat{x}	– estimation state vector
\tilde{x}	– error estimation state vector
u	– input vector
d	– disturbance vector
C	– output matrix
A	– linear matrix
y	– output vector
\tilde{y}	– NN output
L_i	– number of higher-order connections
n	– the state dimension
w_i	– weight state vector
w_i^*	– ideal weight vector
e	– observation error
P_i	– weight estimation error covariance matrix
Q_i	– NN weight estimation noise covariance matrix

R	– Euclidian space
R_i	– error noise covariance
μ_i	– membership value
t	– time, d
RT	– ratio between biomass and substrate

Abbreviations

WWTP	– wastewater treatment plant
RHONN	– recurrent high order neural network
RHONO	– recurrent high order neural observer
NN	– neural network
EKF	– extended Kalman filter
TSS	– total suspended solids
COD	– chemical oxygen demand
BOD	– biological oxygen demand
MIMO	– multiple input multiple output
PI	– proportional – integral controller

References

1. Olsson, G., Wastewater Treatment Systems, Diagnosis and Control, IWA Publishing, London, England, 1999.
2. Brdys, M. A., Urban Water Journal **2** (2005) 125.
3. Vera, G., Sanchez, E. N., Beteau J. F., Proceedings of the American Control Conference **2** (2003) 1836.
4. Tong, R. M., Automatica **16** (1980) 695.
5. Lopez, T., Pulis, A., Revista Mexicana de Ingeniería Química **3** (2004) 51.
6. Alcaraz, V., Gonzalez, V., Robust Nonlinear Observers for Bioprocesses: Application to Wastewater Treatment, Springer-Verlag, Berlin Heidelberg, 2007.
7. Poznyak, A. S., Sanchez, E. N., Yu, W., Differential Neural Networks for Robust Nonlinear Control, World Scientific, Singapore, 2001.
8. Sanchez, E. N., Alanis, A. Y., Loukianov, G., Discrete-Time Recurrent High Order Neural Observer for Induction Motors, Eds. P. Melin, Springer-Verlag, Berlin Heidelberg, Germany, 2007.
9. Rovithakis, G. A., Adaptive Control with Recurrent High-Order Neural Network, Springer-Verlag, New York, USA, 2000.
10. Sanchez, E. N., Alanis, A. Y., Chen, G., Proceedings of Asia-Pacific Workshop on Chaos Control and Synchronization, Melbourne, Australia, 2004.
11. Beteau, J. F., Olsson, G., Jens, A., The COST simulation benchmark: description and simulator manual, European Control Conference, Germany, 2000.
12. Takács, I., Water Res. **25** (1991) 1263.
13. Song, Y., Journal of Mathematical Systems, Estimation and Control **5** (1995) 59.
14. Passino, K., Yurkovich, S., Fuzzy Control, Addison Wesley Longman, INC., New York, USA, 1998.
15. Hamed, M., Environmental Modeling & Software **19** (2004) 919.
16. Marino, R., IEEE Transactions on Automatic Control **35** (1990) 1054.